Hybrid Pd/Fe$_3$O$_4$ nanowires: Fabrication, characterization, optical properties and application as magnetically reusable catalyst for the synthesis of *N*-monosubstituted ureas under ligand-free conditions

Mahmoud Nasrollahzadeh[*,a] Abbas Azarian,[b] Ali Ehsani,[a] S. Mohammad Sajadi[c] and Ferydon Babaei[b]

[a]*Department of Chemistry, Faculty of Science, University of Qom, Qom 37185-359, Iran*

[b]*Department of Physics, University of Qom, Qom, Iran*

[c]*Department of Petroleum Geoscience, Faculty of Science, Soran University, PO Box 624, Soran, Kurdistan Regional Government, Iraq*

ABSTRACT

This paper reports the synthesis and use of Pd/Fe$_3$O$_4$ nanowires, as magnetically separable catalysts for ligand-free amidation coupling reactions of aryl halides with benzylurea under microwave irradiation. Then, the in Situ hydrogenolysis of the products was performed to afford the *N*-monosubstituted ureas in good to excellent yields. This method has the advantages of high yields, simple methodology and easy work up. The catalyst can be recovered by using a magnet and reused several times without significant loss of its catalytic activity. The catalyst was characterized using the powder XRD, SEM, EDS and UV-Vis spectroscopy. Experimental absorbance spectra compared with results from the Gans theory.

Keywords: Metals, Nanostructures, Optical materials, Optical properties

1. Introduction

[*]Corresponding author. Tel.: +98 25 32850953; Fax: +98 25 32103595.

E-mail address: mahmoudnasr81@gmail.com (M. Nasrollahzadeh).

N-Monosubstituted urea compounds constitute a very important class of organic compounds playing a significant role in a number of natural products and bioactive molecules [1-4].

The classical approaches to substituted ureas are based on the reaction of primary amines with toxic phosgene or its derivatives [5,6], reaction of primary or secondary amines with isocyanates or reaction with sodium or potassium cyanate in aqueous solution in the presence of one equivalent of HCl [7,8], insertion of CO or CO_2 into amino compounds in the presence of different catalysts in organic solvents (at high pressure and temperature) [9-12], acid or base-catalyzed hydration of cyanamides or reaction of *S,S*-dimethyl dithiocarbonate with ammonia in water-dioxane [13-16].

However, each of these methods suffer from different drawbacks such as employing expensive, toxic, hazardous and moisture sensitive reagents, harsh reaction conditions, tedious work-ups, long reaction times, low yields, several-step methods, environmental pollution caused by formation of side products [13-16]. Thus, due to safety considerations, it is desirable to develop a more efficient and convenient method for the synthesis of *N*-monosubstituted ureas that reduce or eliminate the use and generation of hazardous compounds is essential.

Palladium-catalyzed C-N cross-coupling reactions have evolved into a highly versatile and synthetically attractive technique for targeting pharmaceutically useful intermediates [17-19]. While a number of C-N cross-coupling methods to synthesize symmetrical and unsymmetrical diarylureas exist, methods for the formation of monoarylureas are sparse [20,21]. As an alternative approach, we believed a mild and efficient cross-coupling method might be utilized to greatly expand the inventory of available monoarylureas.

Nanotechnology is emerging as a cutting edge technology interdisciplinary with biology, chemistry and material science. Metal nanoparticles have been used widely in recent years due to their unique electronic, optical, mechanical, magnetic and chemical properties which differ greatly from the bulk substances [22]. For these reasons, metallic nanoparticles have found uses in many applications in different fields, such as catalysis, photonics, and electronics. Palladium (Pd) is able to catalyze a wide variety of chemical reactions homogeneous and heterogeneous under conditions and therefore it is one of the most widely used metal catalysts [23]. Due to a higher available catalytic surface, heterogeneous catalysts are more and more used in the form of nanoparticles. Recently, a variety of magnetic nanoparticles amenable for easy separation and recovery have been synthesized and applied as heterogeneous catalysts to a range of chemical reactions [24-27].

In the course of our researches on the applications of heterogeneous catalysts [28-35], herein we report a new, simple and inexpensive protocol for the preparation of Pd/Fe$_3$O$_4$ nanowires by arc discharge of Fe in deionized (DI) water and simple drop drying deposition of palladium. The main advantage of the present method is the direct formation of Fe nanowires from discharge of Iron electrodes within water. The catalyst is heterogeneous and reusable, which provides an advantage over the homogeneous Pd-catalyst.

Several methods for preparation of Fe nanowires have been reported, but synthetic approaches for these materials are needed. Classical methods for the synthesis of Fe nanowires have involved epitaxy [36], chemical deposition [37], self-assembly [38] and electrochemical method [39]. In spite of these methods, there are no reports on the preparation of iron nanowires by electrical arc discharge method. The early works by arc discharge method in liquids were based on production of carbonaceous nanostructures such as MWCNTs, SWCNTs, SW-CNHs and nano onions [40-43]. In general, electrical arc

discharge in water has the advantage in this regard as it produces self-crystallized nanoparticles due to high temperature caused by joule heating. Moreover, compared with other techniques, electrical arc discharge in water is an attractive method because of simplicity of experimental set up, lack of need for complicated equipment, low impurity, less production steps leading to a high-throughput and cost-effective procedure to generate a high yield of nanoparticles.

In the next step, we hereby describe the development of Pd/Fe_3O_4 nanowires as a novel and stable heterogeneous catalyst for the amidation of aryl halides with benzylurea (Scheme 1). The amidation of aryl halides with benzylurea, followed by hydrogenolysis, provides the corresponding *N*-monosubstituted ureas in high yield.

Scheme 1.

During this study, we also introduce the effective medium optical constant for decorated nanowires (Fe_3O_4 nanowires decorated by Pd nanoparticles) thin films by comparing the experimental data and calculation results in the spectral range of 300-700 nm. Gans theory and these effective optical constants were used for calculation of extinction cross section of dispersed above nanostructures in water. Our simulation results show that this approach can be used for prediction of optical spectra of decorated nanowires.

2. Experimental

2.1. Instruments and reagents

All reagents were purchased from the Merck and Aldrich chemical companies and used without further purification. Products were characterized by different spectroscopic methods (FT-IR and ^{1}H NMR spectra), elemental analysis (CHN) and melting points. The NMR spectra were recorded in acetone and DMSO. ^{1}H NMR spectra were recorded on a Bruker

Avance DRX 250, 300 and 400 MHz instrument. The chemical shifts (δ) are reported in ppm relative to the TMS as internal standard. *J* values are given in Hz. IR (KBr) spectra were recorded on a Perkin-Elmer 781 spectrophotometer. Melting points were taken in open capillary tubes with a BUCHI 510 melting point apparatus and were uncorrected. The elemental analysis was performed using Heraeus CHN-O-Rapid analyzer. TLC was performed on silica gel polygram SIL G/UV 254 plates. X-ray diffraction measurements were performed with a Philips powder diffractometer type PW 1373 goniometer. It was equipped with a graphite monochromator crystal. The X-ray wavelength was 1.5405 A• and the diffraction patterns were recorded in the 2 range (10-60) with scanning speed of 2º/min. Morphology and particle dispersion was investigated by scanning electron microscopy (SEM) (Cam scan MV2300). The chemical composition of the prepared nanostructures was measured by EDS performed in SEM. UV-Visible spectral analysis was recorded on a double-beam spectrophotometer (Hitachi, U-2900).

2.2. Preparation of Fe₃O₄@Pd nanowires

For fabrication of Fe nanowires we used the preparation system consisted of two main parts: a high current DC power supply and a reactor including an anode, cathode and a micrometer which moves the anode in contact with cathode. In this method, an 8 V DC voltage and 5 A current are applied between two metallic iron electrodes; it was found that the voltage dropped to 5 V during the arc formation but the current remained constant. Both anode and cathode were Fe, wire shaped, 2 mm in diameter and 99.99% purity. Initially we bring the two electrodes into contact, leading to a small contact cross section and thus to a high current density. As more Iron is ablated from the anode, the plasma expands, pushing the liquid away, and a gaseous bubble forms. Melted species can react with plasma and then condense into the liquid. In order to extract the dispersed wires, the solution was dried at a

pressure of 10^{-1} Torr and centrifuged several times and then dispersed on glass substrate. Deposition of Pd on surface of Fe nanowires was accomplished via a simple drop-drying process by dropping $PdCl_2$ solution onto Fe nanowires films and drying them at room temperature. This solution was prepared by ultrasonically solving a 0.02 g $PdCl_2$ powder (5 N), 99.9 mL DI water and 0.1 mL HCl. Next to the Pd deposition, samples were washed with DI water several times and then dried in air. However, Fe nanowires are very air-sensitive and easily oxidized to Fe_3O_4 nanowires in water.

2.3. General experimental procedure for the synthesis of N-monosubstituted ureas

A Smith process vial was charged with 1.0 mol% Pd/Fe_3O_4 nanowires, 1.0 mmol of phenylurea, 1.0 mmol of aryl halide and Cs_2CO_3 (1.5 mmol). After sealing the cap and twice purging with N_2, the vial was irradiated by microwave at 120 °C for 1 h in the Smith Synthesizer. After completion of the reaction (as monitored by TLC), the reaction mixture was cooled to room temperature, and a small volume of MeOH (4 mL) was added, the catalyst was separated by a magnetic separator and the reaction mixture was filtered through a pad of Celite and MeOH (6 mL/mmol), conc. HCl and an equal weight of Pd black were added and the reaction vessel is connected to a Parr medium pressure hydrogenation apparatus (40-50 psi) then was stirred at room temperature for 20 h.

The mixture was quenched with 2 M NaOH, filtered, diluted with 30 mL of ethyl acetate and washed with 2 M NaOH. Then the mixture was extracted three times with ethyl acetate (30 mL each). The organic layer was dried over Na_2SO_4 and the solvent was removed under reduced pressure. The residue was subjected to gel permeation chromatography to afford pure products.

The elemental analysis (CHN), IR, ^{1}H NMR and ^{13}C NMR data of the unknown substituted ureas is given as below:

_N_-(2,5-Dichlorophenyl)urea (Table 1, entry 4):

White color; Yield 87%; M.p. 222-224 °C; FT-IR (KBr, cm^{-1}) 3495, 3417, 3364, 3340, 3308, 3206, 2826, 1676, 1610, 1586, 1535, 1466, 1410, 1385, 1351, 1263, 1089, 1056, 873, 805, 792, 764, 583, 557, 475, 440, 418; ^{1}H NMR (300 MHz, DMSO-d_6) δ_H = 8.24 (s, 2H), 7.38 (d, J = 8.1 Hz, 1H), 6.96 (d, J = 8.1 Hz, 1H), 6.55 (s, 2H); ^{13}C NMR (75 MHz, DMSO-d_6) δ_C = 154.7, 137.7, 131.7, 129.9, 121.5, 119.5, 118.8; Anal. Calcd for $C_7H_6N_2OCl_2$: C, 41.00; H, 2.95; N, 13.66. Found: C, 39.84; H, 2.89; N, 13.80.

_N_-(4-Acethylphenyl)urea (Table 1, entry 5):

White color; Yield 85%; M.p. 297-298 °C; FT-IR (KBr, cm^{-1}) 3407, 3307, 3215, 1672, 1613, 1584, 1536, 1508, 1410, 1357,1310, 1273, 1117, 1013, 963, 874, 835, 766, 747, 718, 632, 655, 594, 494, 410; ^{1}H NMR (300 MHz, DMSO-d_6) δ_H = 8.93 (s, 1H), 7.80 (d, J = 8.4 Hz, 2H), 7.50 (d, J = 8.4 Hz, 2H), 6.02 (s, 2H), 2.47 (s, 3H); ^{13}C NMR (75 MHz, DMSO-d_6) δ_H = 196.6, 156.0, 145.7, 130.2, 130.0, 117.0, 26.7; Anal. Calcd for $C_9H_{10}N_2O_2$: C, 60.66; H, 5.66; N, 15.72. Found: C, 60.47; H, 5.45; N, 15.59.

_N_-(1-Naphthyl)urea (Table 1, entries 6 and 7):

White color; Yield 82%; M.p. 221-222 °C; FT-IR (KBr, cm^{-1}) 3444, 33055, 3206, 3052, 2922, 1651, 1608, 1555, 1530, 1505, 1360, 1335, 1278, 1101, 785, 772, 608, 530; ^{1}H NMR (250 MHz, DMSO-d_6) δ_H = 8.70 (s, 1H), 8.17 (s, 1H), 8.00 (d, J = 7.3 Hz, 1H), 7.85 (s, 1H), 7.73-7.37 (m, 4H), 6.22 (s, 2H); ^{13}C NMR (62.5 MHz, DMSO-d_6) δ_C = 157.1, 135.9, 134.5, 128.9, 126.6, 126.4, 126.0, 122.7, 122.3, 117.5; Anal. Calcd for $C_{11}H_{10}N_2O_2$: C, 70.95; H, 5.41; N, 15.04. Found: C, 70.82; H, 5.34; N, 14.91.

_N_-(2-Methylphenyl)urea (Table 1, entries 8 and 9):

White color; Yield 87%; M.p. 196-198 °C; FT-IR (KBr, cm^{-1}) 3438, 3315, 3218, 1650, 1613, 1582, 1547, 1459, 1354, 1289, 1258, 1117, 1041, 844, 747, 596, 480; ^{1}H NMR (250 MHz,

DMSO-d_6) δ_H = 7.79 (t, J = 6.4 Hz, 1H), 7.69 (s, 1H), 7.13-7.07 (dd, J = 8.0 Hz, J = 7.6 Hz, 2H), 6.88 (d, J = 7.4 Hz, 1H), 6.03 (s, 2H), 2.19 (s, 3H); ^{13}C NMR (62.5 MHz, DMSO-d_6) δ_H = 156.6, 138.6, 130.5, 127.4, 126.4, 122.5, 121.4, 18.36; Anal. Calcd for $C_8H_{10}N_2O$: C, 63.98; H, 6.71; N, 18.65. Found: C, 63.85; H, 6.61; N, 18.52.

3. Results and discussion

3.1. Characterization of catalyst

The catalyst was characterized using the powder XRD, SEM, EDS and UV-Vis spectroscopy.

Fe_3O_4 nanowires decorated by Pd nanoparticles (FNDP) were fabricated by two-step simple synthesis process. Fe_3O_4 nanowires with several micron lengths were synthesized through arc discharge of iron electrodes in DI water and then they were dispersed on glass substrates and dried in air. Palladium nanoparticles were overlaid on surface of Fe_3O_4 nanowires via a simple drop-drying process by dropping $PdCl_2$ solution onto Fe nanowires films and drying them at room temperature. Figure 1 illustrates typical morphologies of Fe_3O_4 nanowires obtained at 5 A arc currents. In general Fe tends to form wire-like structures due to its lattice geometry. The presence of a high temperature region and DI water in the reactor leads to the formation of a temperature gradient and fast condensation process. In fact rapid cooling of the products reduces the growth rate of the created nuclei and they do not have enough time to form wire-shape structures before stabilization. Hence, there are also other shapes than nanowires in our samples, which is due to fast condensation. Scanning electron microscopy images illustrate Fe_3O_4 nanowires with range size from 1 to less than 20 µm length and about 100 nm diameter. Figure 2 shows typical Back scattering electrons (BSE) mode of SEM micrograph of samples after Pd nanoparticles shell deposition. BSE

8

mode permits having a contrast between elements with different atomic numbers. Hence, Pd particles appear as bright dots over the surface of Fe_3O_4 nanowires with average size less than 30 nm.

Figure 1.

Figure 2.

The crystalline structure and phase composition of catalyst was confirmed by X-ray diffraction measurement. The X-ray diffraction pattern revealed that Fe nanoparticles are very oxygen-sensitive and easily oxidized to Fe_3O_4 (Figure 3). All of the peaks in the X-ray diffraction (XRD) pattern could also be assigned to the corresponding lattice planes of face-centered-cubic (fcc) Pd and Fe_3O_4 crystals in accordance with the bimetallic heterodimer structure.

Figure 3.

We used Energy Dispersive X-ray Spectroscopy (EDS) to determine chemical composition of our samples. In the EDS spectrum of catalyst, peaks related to O, Fe and Pd were observed. The atomic and weight ratios are listed in Table 1. The excess oxygen is due to physical absorption of oxygen from environment during sample preparation.

Table 1.

3.2. Optical Properties

For non-spherical metallic particles, to calculate the light absorption by them, the orientation with respect to the oscillating electric field must be taken in to account. In 1912, Gans derived the extinction cross-section for nanowires, when the dipole approximation holds [44].

In recent years, many papers have been published about surface plasmon resonance (SPR) of nanowires. In most of these articles the Gans theory widely used because SPR properties of nanowires is in good agreement with the results of this theory [45].

In this work, we introduce the effective medium optical constant of these thin films by comparing the experimental data and calculation results and then Gans theory which these optical constants were used for calculation of extinction cross section of dispersed Fe nanowires decorated by Pd nanoparticles in water. A typical UV-Vis spectrum of the FNDP thin films on glass substrates is shown in Figure 4.

Figure 4.

In order to obtain the real part of refraction indices (n_f) of the Pd/Fe_3O_4 thin films, we have used the prescription given in [46,47] where it is suggested that the following equation may be used to obtain the optical constants of low absorption thin films:

$$T = \frac{16 n_0 n_s n_f^2 \alpha_{ext}}{C_1^2 + C_2^2 \alpha_{ext}^2 + 2 C_1 C_2 \alpha_{ext} COS(4\pi n_f d / \lambda)} \qquad (1)$$

$$C_1 = (n_0 + n_f)(n_f + n_s) \qquad (2)$$

$$C_1 = (n_0 - n_f)(n_f - n_s) \qquad (3)$$

$$\alpha_{ext} = \exp(-4\pi K d / \lambda) \qquad (4)$$

Where, n_0, n_s, n_f are real parts of the refraction indices of the thin film, the substrate and the air, respectively. Moreover, d is the film thickness and K is the imaginary part of the refraction index of Pd/Fe_3O_4 thin films. To obtain the values of K, using the extinction coefficient equation as [48]:

$$\alpha_{ext} = \exp(-4\pi k d / \lambda) = \frac{T}{1 - R} \qquad (5)$$

The effective real and imaginary parts of refraction indices of Pd/Fe$_3$O$_4$ thin films are shown in Figure 5. We used these effective values as input data at Gans theory for calculation of extinction cross section of dispersed Pd/Fe$_3$O$_4$ in water.

Figure 5.

Details of the Gans theory can be found in literature [49]. According to the Gans theory, the extinction coefficient γ for N particles of volume V is given by the following equation.

$$\gamma = \frac{2\pi N V \varepsilon_m^{3/2}}{3\lambda}\left[\frac{\frac{2}{p_x^2}\varepsilon_2}{(\varepsilon_1 + k_x\varepsilon_m)^2 + \varepsilon_2^2} + \frac{\frac{1}{p_z^2}\varepsilon_2}{(\varepsilon_1 + k_z\varepsilon_m)^2 + \varepsilon_2^2}\right] \tag{6}$$

Where λ the wavelength of the light, ε_m the dielectric constant of the medium and ε_1 and ε_2 the real and complex part of copper dielectric function related to interacting light.

In this theory for each dimension a geometrical factor (P_i) are given by

$$p_z = \frac{1-e^2}{e}\left(\frac{1}{2e}\ln\left(\frac{1+e}{1-e}\right)-1\right) \tag{7}$$

$$p_x = p_y = \frac{1}{2}(1 - p_z) \tag{8}$$

$$e = \frac{\sqrt{L^2 - d^2}}{L} \tag{9}$$

Where, L and d is the nanowires length and diameter, respectively. For each dimension the screening parameter is

$$K_i = \frac{1}{p_i}(1 - p_i) \tag{10}$$

Here K_i (i =1, 2, 3) are the same K_X, K_Y and K_Z in equation (6). The result of this process is shown at Figure 6. It is clear that there is good agreement between calculation and experimental values of absorption spectra of Pd/Fe$_3$O$_4$ dispersed in water.

11

Figure 6.

3.3. Activity of Pd/Fe$_3$O$_4$ nanowires catalyst for the preparation of N-monosubstituted ureas

The catalytic behavior of the Pd/Fe$_3$O$_4$ nanowires was studied for the synthesis of *N*-monosubstituted ureas. Reaction conditions were optimized for the amidation reaction using 2,5-dichlorobromobenzene as a substrate, benzylurea and Pd/Fe$_3$O$_4$ nanowires as heterogeneous catalysts in the presence of various bases under microwave conditions at 120 °C (Table 2). Control experiments show that there is no effective reaction in the absence of catalyst (Table 2, entry 6). However, addition of the Pd/Fe$_3$O$_4$ nanowires to the mixture has rapidly increased the amidation of aryl halides in high yields. Our experiments showed that the base was necessary for the amidation reaction. Among the selected bases, Cs$_2$CO$_3$ acted as the most effective one (Table 2, entry 1). Reaction without base did not give any product. The effect of catalyst loading was probed. Catalyst loads of 1.0 mol % were typically required to achieve quantitative conversion with most substrates. The use of lower catalyst loadings resulted in incomplete reactions (entry 8).

We then used the optimal reaction conditions (catalyst (1.0 mol %), aryl halide (1.0 mmol), benzylurea (1.0 mmol) and Cs$_2$CO$_3$ (1.5 mmol)) for amidation of different aryl halides under microwave conditions at 120 °C) for 1 h and the results are shown in Table 3. Then, the in Situ hydrogenolysis of 1-benzyl-3-arylureas in MeOH and in the presence of conc. HCl and Pd black yield the desired *N*-monosubstituted ureas in good to excellent yields.

Table 2.

To study the effects of the nature of the substituents, various 1-benzyl-3-arylureas were synthesized from the reaction between different aryl halides containing both electron-releasing and electron-withdrawing groups with benzylurea in good to excellent yields. As

12

shown in Table 3, 1-bromo and 1-iodonaphthyl gave the corresponding adduct in good yield (Table 2, entries 6 and 7).

Table 3.

To the best of our knowledge, Pd/Fe_3O_4 nanowires are one of the most general and active catalysts reported so far for the synthesis of *N*-monosubstituted ureas. These results represent a significant advancement in the C-N coupling reaction. Although the mechanism of Pd-catalyzed coupling is not obvious and further studies to elucidate the detailed reaction mechanism are ongoing in our laboratory. It should be noted that Pd/Fe_3O_4 nanowires were absolutely necessary for this reaction as verified by a control experiments where no reaction occurred in the absence of Pd/Fe_3O_4 nanowires or in the presence of only Fe_3O_4 even at a higher reaction temperature for a prolonged reaction time. Based on the most accepted coupling reaction mechanism, Pd nanoparticles are expected to be the reasons for the high catalytic activity of the catalyst Pd/Fe_3O_4 in comparison with Fe_3O_4. In the other word, the high activity of Pd/Fe_3O_4 catalyst for the synthesis of *N*-monosubstituted ureas could be attributed to the formation of small active Pd nanoparticles on the surface of Fe_3O_4.

After removal of the solvent and purification, the products were characterized by melting points, elemental analysis (CHN), IR, ^1H NMR and ^{13}C NMR. Appearance of the two absorption bands in the range of 3200-3400 cm^{-1} (NH stretching bands) and one absorption band in the range of 1640-1670 cm^{-1} (C=O) in the IR spectrum confirmed formation of the *N*-monosubstituted ureas. The ^1H NMR spectra of the products showed one NH proton signal and another signal for the NH_2 protons. The ^{13}C NMR spectra of the products showed one signal for the carbonyl carbon.

3.4. Catalyst recyclability

The reusability of the catalyst was checked in the reaction of benzylurea with iodobenzene under the present reaction conditions (Table 3, entry 4). After the completion of the reaction, the insoluble catalyst was separated from the reaction mixture by the application of an external magnet. The catalyst was washed with ethyl acetate several times, dried in a hot air oven at 100 °C for 2 h and employed for the next reaction. The catalytic activity did not decrease considerably after four catalytic cycles. The reusability of the catalysts is one of the most important benefits and makes them useful for commercial applications.

4. Conclusions

In conclusion we have developed an efficient protocol for the preparation of Pd/Fe_3O_4 nanowires. The catalyst was characterized by SEM, XRD, EDS and UV-Vis spectroscopy and exhibited good activities in ligand-free coupling reactions of aryl halides with benzylurea. This system allows the coupling of electron-rich, -neutral, and -deficient aryl halides in good to excellent yields. This method has the advantages of high yields, elimination of homogeneous catalysts, simple methodology and easy work up. The catalyst is eco-friendly catalyst because it produces little waste, and can be recovered by a magnet and successively reused without the significant loss of activity. Also, the optical properties of the catalyst were also studied.

Acknowledgments

References

[1] K. Matsuda, Med. Res. Rev. 14 (1994) 271.

[2] N.N. Melnikov, In Chemistry of Pesticides; Gunther, J.D., Ed.; Springer-Verlag: Berlin, 1971, 225.

[3] A. Tsopmo, D. Ngnokam, D. Ngamga, J.F. Ayafor, O. Sterner, J. Nat. Prod. 62 (1999) 1435.

[4] Y. Funabashi, S. Tsubotani, K. Koyama, N. Katayama, S. Harada, Tetrahedron 49 (1993) 13.

[5] V. Papesch, E.F. Schroeder, J. Org. Chem. 16 (1951) 1879.

[6] R.L. Clark, A.A. Pessolano, J. Am. Chem. Soc. 80 (1958) 1658.

[7] E.A. Jefferson, E.E. Swayze, Tetrahedron Lett. 40 (1999) 7757.

[8] S. Knapp, J.J. Hale, M. Bastos, A. Molina, K. Y. Cheng, J. Org. Chem. 57 (1992) 6239.

[9] X. Peng, F. Li, C. Xia, Synlett (2006) 1161.

[10] B. Zhu, R.J. Angelici, J. Am. Chem. Soc. 128 (2006) 14460.

[11] Y. Nishiyama, H. Kawamatsu, N. Sonoda, J. Org. Chem. 70 (2005) 2551.

[12] F. Bigi, R. Maggi, G. Sartori, Green Chem. 2 (2000) 140.

[13] V. D. Jadhav, E. Herdtweck, F.P. Schmidtchen, Chem. Eur. J. 14 (2008) 6098.

[14] D. Schade, K. Topker-Lehmann, J. Kotthaus, B. Clement, J. Org. Chem. 73 (2008) 1025.

[15] E. Artuso, I. Degani, R. Fochi, C. Magistris, Synthesis (2007) 3497.

[16] S.H. Kim, B.R. Park, J.N. Kim, Bull. Korean Chem. Soc. 32 (2011) 716.

[17] S.A. Lawrence, Amines, Synthesis Properties, and Application. Cambridge University Press, Cambridge, 2004.

[18] S. Breitler, N.J. Oldenhuis, B.P. Fors, S.L. Buchwald, Org. Lett. 13 (2011) 3262.

[19] A.G. Sergeev, G.A. Artamkina, I.P. Beletskaya, Russ. J. Org. Chem. 38 (2002) 538.

[20] B.J. Kotecki, D.P. Fernando, A.R. Haight, K.L. Lukin, Org. Lett. 11 (2009) 947.

[21] A.G. Sergeev, G.A. Artamkina, V.S. Velezheva, I.N. Fedorova, I.P. Beletskaya, Russ. J. Org. Chem. 41 (2005) 860.

[22] M.C. Daniel, D. Astruc, Chem. Soc. Rev. 104 (2004) 293.

[23] A. Molnar, Chem. Rev. 111 (2011) 2251.

[24] M.A. Willard, L.K. Kurihara, E.E. Carpenter, S. Calvin, V.G. Harris, Int. Mater. Rev. 49 (2004) 125.

[25] M. Zhu, G. Diao, J. Phys. Chem. C 115 (2011) 24743.

[26] M. Zhu, C. Wang, D. Meng, G. Diao, J. Mater. Chem. A 1 (2013) 2118.

[27] M. Zhu, G. Diao, Nanoscale 3 (2011) 2748.

[28] P. Fakhri, B. Jaleh, M. Nasrollahzadeh, J. Mol. Catal. A: Chem. 383-384 (2014) 17.

[29] D. Habibi and M. Nasrollahzadeh, H. Sahebekhtiari, J. Mol. Catal. A: Chem. 378 (2013) 148.

[30] M. Nasrollahzadeh, A. Ehsani, A. Rostami-Vartouni, Ultrason. Sonochem. 21 (2014) 275.

[31] A. Ehsani, F. Babaei, M. Nasrollahzadeh, Appl. Surf. Sci. 283 (2013) 1060.

[32] A.R. Modarresi-Alam, M. Nasrollahzadeh, F. Khamooshi, Sci. Iran. 15 (2008) 452.

[33] D. Habibi, S. Heydari, M. Nasrollahzadeh, J. Chem. Res. 36 (2012) 573.

[34] D. Habibi, M. Nasrollahzadeh, L. Mehrabi, S. Mostafaee, Monatsh. Chem. 144 (2013) 725.

[35] A. Ehsani, S. Adeli, F. Babaei, H. Mostaanzadeh, M. Nasrollahzadeh, J. Electroanal. Chem. 713 (2014) 91.

[36] H.M. Hwang, J. H. Kang, J. Lee, J.Y. Choi, H.H. Lee, Electrochem. Solid-State Lett. 11 (2008) K7.

[37] W-S. Lin, Z.-J. Jian, H.-M. Lin, L.-C. Lai, et all, J. Chin. Chem. Soc. 60 (2013) 85.

[38] D.J. Sellmyer, M. Zheng, R. Skomski, J. Phys. Condens. Matter. 13 (2001) R433.

[39] J. Zhang, W. M. Tong, H. Ding, H.B. Wang, H. Wang, Integrated Ferroelectrics, 141 (2013) 24.

[40] I. Alexandrou, H. Wang, N. Sano, G.A.J. Amaratunga, J. Chem. Phys. 120 (2004) 1055.

[41] D. Bera, G. Johnston, H. Heinrich, S. Seal Nanotechnology 17 (2006) 1722.

[42] D. Bera, S.C. Kuiry, M. McCutchen, S. Seal, H. Heinrich, G. C. Slane J. Appl. Phys. 96 (2004) 5152.

[43] N. Sano, Mater. Chem. Phys. 88 (2004) 235.

[44] R. Gans, Ann. Phys. 37 (1912) 881.

[45] S. Eustis, M. El-Sayed, J. Phys. Chem. B 109 (2005) 16350.

[46] S.Z. Shang, K. Yi, Z.X. Fan, Appl. Surf. Sci. 242 (2005) 437.

[47] S. Wang, X. Fu, G. Xia, J. Wang, J. Shao, and Z. Fan, Appl. Surf. Sci. 252 (2006) 8734.

[48] J.R. Reitz, F. J. Milford, Foundations of Electromagnetic Theory (Reading, MA: Addison-Wesley) 1960.

[49] C.F. Bohren, D. R. Huffman, Absorption and Scattering of Light by Small Particles, John Wiley & Sons, New York, 1983.

Scheme caption

Scheme 1. Synthesis of *N*-monosubstituted ureas.

X: I & Br
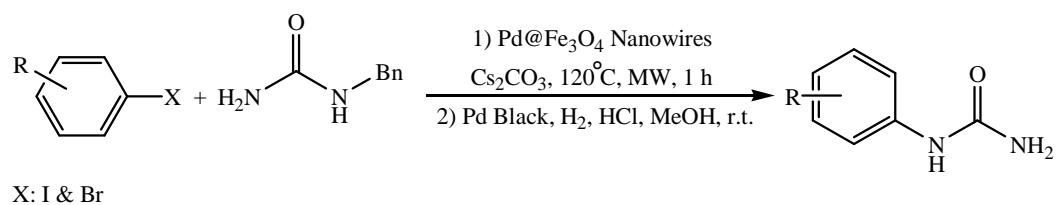
Scheme 1. Synthesis of *N*-monosustituted ureas

Figure captions

Figure 1. Typical SEM image of Fe nanowires prepared at 5 A electrical arc currents.

Figure 2. Typical SEM image of samples after deposition of Pd.

Figure 3. XRD pattern of Pd/Fe$_3$O$_4$ nanowires.

Figure 4. A typical UV-Vis absorption spectrum of the Pd/Fe$_3$O$_4$ thin films on glass substrates.

Figure 5. Investigated effective optical constants of Pd/Fe$_3$O$_4$.

Figure 6. Experimental and calculated absorption spectra by effective optical constants of Pd/Fe$_3$O$_4$ dispersed in water.

Figure 1. Typical SEM image of Fe nanowires prepared at 5 A electrical arc currents.
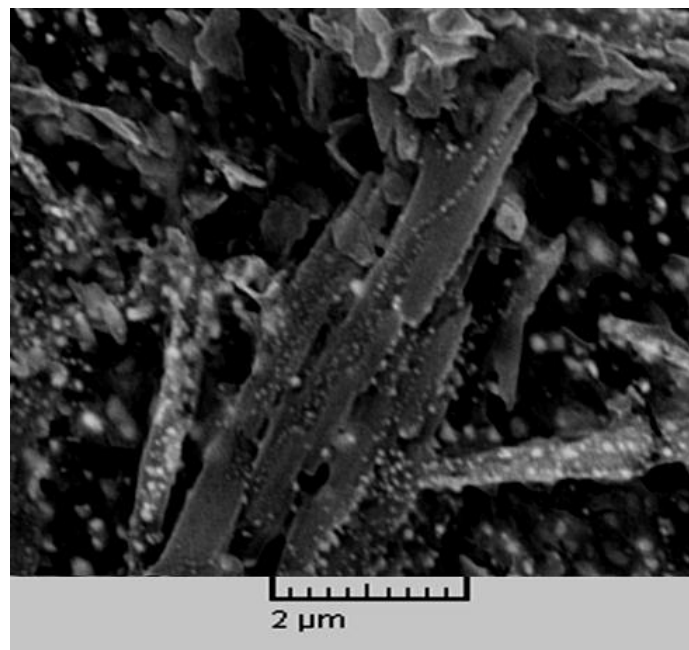
Figure 2. Typical SEM image of samples after deposition of Pd.
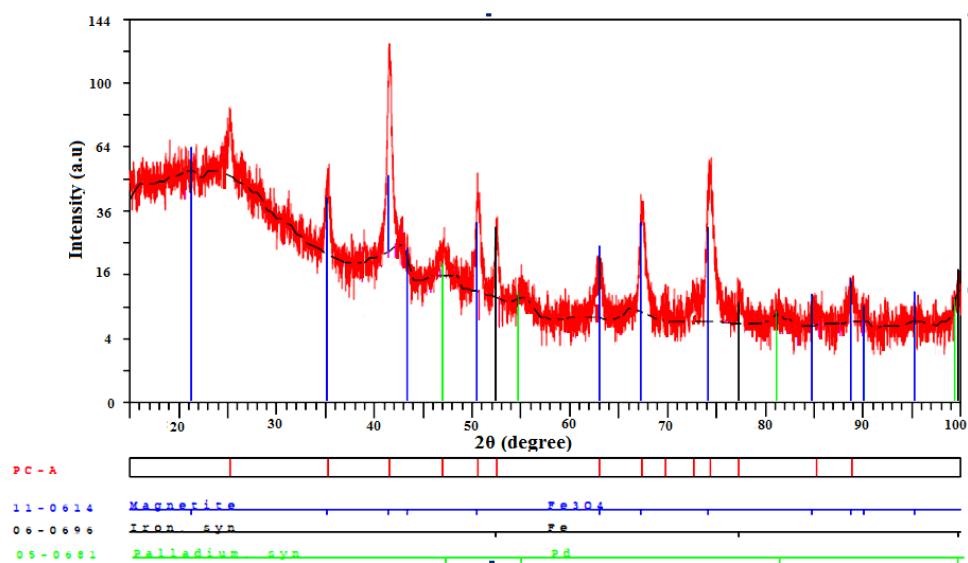
Figure 3. XRD pattern of Pd/Fe$_3$O$_4$ nanowires.
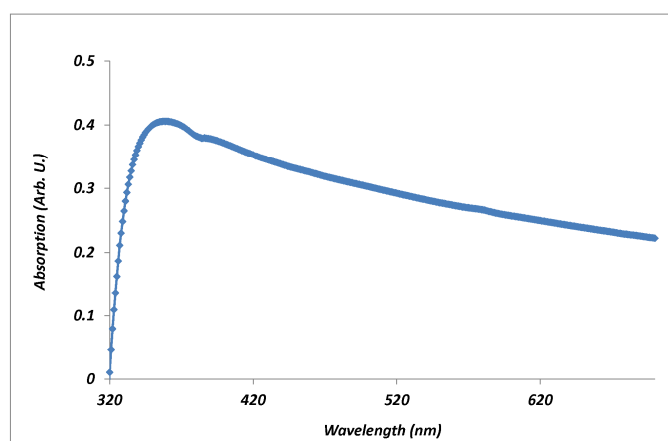
Figure 4. A typical UV-Vis absorption spectrum of the Pd/Fe$_3$O$_4$ thin films on glass substrates.
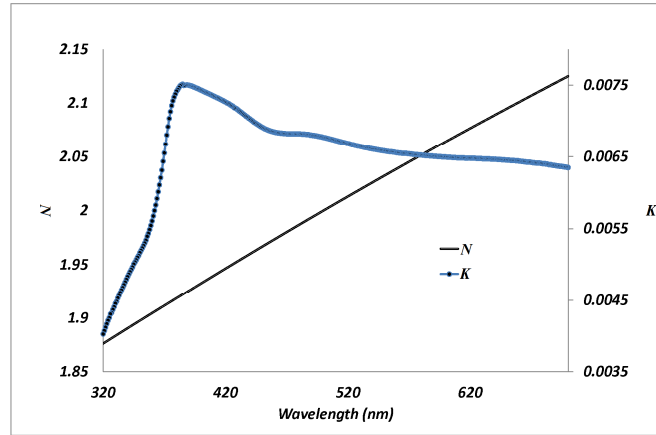
Figure 5. Investigated effective optical constants of Pd/Fe$_3$O$_4$.
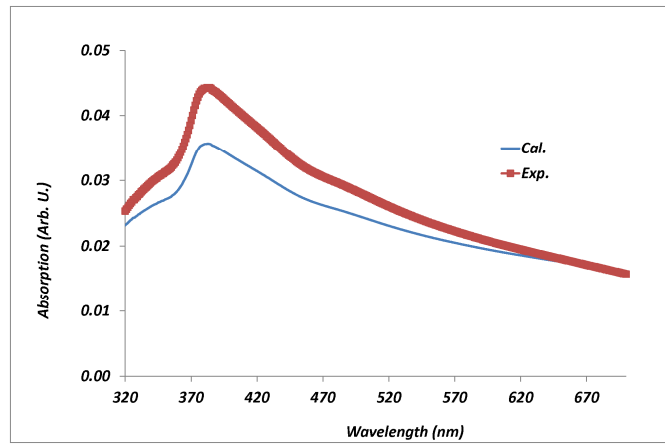
Figure 6. Experimental and calculated absorption spectra by effective optical constants of Pd/Fe$_3$O$_4$ dispersed in water.

Table captions

Table 1. Atomic and weight ratios of Pd/Fe$_3$O$_4$.

Table 2. Optimization of reaction conditions in amidation reaction of 2,5-dichlorobromobenzene with benzylurea.

Table 3. Formation of *N*-monosubstituted ureas.

Table 1.

Atomic and weight ratios of Pd/Fe$_3$O$_4$.

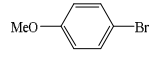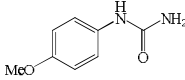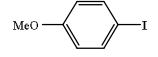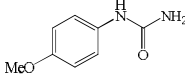| Element	Series	Norm. C [wt %]	Atom. C [at %]
Iron	K series	26.07	9.00
Palladium	K series	6.18	1.12
Oxygen	K series	42.35	51.05
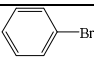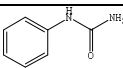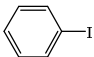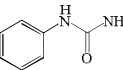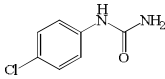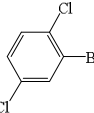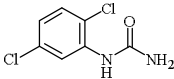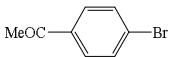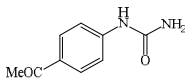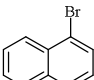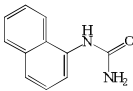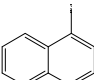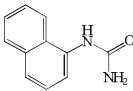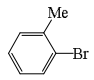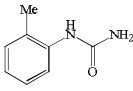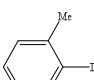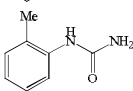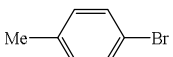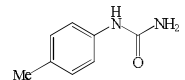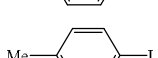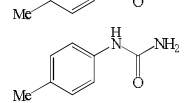
Table 2.

Optimization of reaction conditions in amidation reaction of 2,5-dichlorobromobenzene with benzylurea.[a]

Entry	Pd/Fe$_3$O$_4$ nanowires (mol %)	Base	Yield[b] (%)
1	1.0	Cs$_2$CO$_3$	89
2	1.0	Na$_2$CO$_3$	50
3	1.0	K$_3$PO$_4$	80
4	1.0	K$_2$CO$_3$	82
5	1.0	0	0
6	0	Cs$_2$CO$_3$	0
7	2.0	Cs$_2$CO$_3$	88
8	0.7	Cs$_2$CO$_3$	72

[a]Reaction condition: 1.0 equiv of aryl halide, 1.0 equiv of benzylurea, 1.0 mol % of catalyst and 1.5 equiv of base, 120 °C, 1 h.

[b]Isolated yield.

Table 3.

Formation of *N*-monosubstituted ureas.

Entry	Aryl halide	Product	Yield [a] (%)	Reference
1			87	16
2			89	16
3			85	16
4			89 (88,88,87)[b]	This work
5			85	This work
6			82	This work
7			85	This work
8			87	This work
9			86	This work
10			84	commercial
11			86	commercial
12			83	16
13			85	16

[a] Yields are after work-up.

[b] Yield after the fourth cycle.

Abbreviations

XRD: X-ray Powder Diffraction

24

SEM: Scanning Electron Microscopy

EDS: Energy Dispersion X-ray Spectroscopy

FT-IR spectroscopy: Fourier transform infrared spectroscopy

NMR: Nuclear Magnetic Resonance